

# Global reconstruction of initial conditions of nonlinear parabolic equations via the Carleman-contraction method

Thuy T. Le\*

## Abstract

We propose a global convergent numerical method to reconstruct the initial condition of a nonlinear parabolic equation from the measurement of both Dirichlet and Neumann data on the boundary of a bounded domain. The first step in our method is to derive, from the nonlinear governing parabolic equation, a nonlinear systems of elliptic partial differential equations (PDEs) whose solution yields directly the solution of the inverse source problem. We then establish a contraction mapping-like iterative scheme to solve this system. The convergence of this iterative scheme is rigorously proved by employing a Carleman estimate and the argument in the proof of the traditional contraction mapping principle. This convergence is fast in both theoretical and numerical senses. Moreover, our method, unlike the methods based on optimization, does not require a good initial guess of the true solution. Numerical examples are presented to verify these results.

*Keywords:* Nonlinear equations, initial condition, inverse source problem, convergent numerical method, Carleman estimate, iteration, contraction mapping

*AMS Classification* 35R30, 35K20

## 1 Introduction

The problem of recovering the initial condition for a nonlinear parabolic equation from the measurement of the Dirichlet and Neumann data in a bounded domain arises in many real-world applications, for example, detecting the pollution on the surface of the rivers or lakes [1], reconstructing of the spatially distributed temperature inside a solid from the heat and the heat flux on the boundary in the time domain [7], effective monitoring heat and conduction processes in steel industries, glass and polymer-forming and nuclear power station [28]. Due to its realistic applications, this inverse source problem has been studied intensively. It is formulated as follows.

Let  $d \geq 1$  be the spatial dimension, let  $\Omega$  be an open and bounded domain in  $\mathbb{R}^d$  with smooth boundary  $\partial\Omega$ , and let  $T$  be a positive number. Let  $F : \mathbb{R}^d \times \mathbb{R} \times \mathbb{R} \times \mathbb{R}^d \rightarrow \mathbb{R}$  and  $c : \mathbb{R}^d \rightarrow [c_0, \infty)$ , for some  $c_0 > 0$ , be functions in the class  $C^1$ . Denote by  $Q_T$  the set  $\Omega \times (0, T)$ .

Consider the function  $u(\mathbf{x}, t)$  is governed by the following problem:

$$\begin{cases} c(\mathbf{x})u_t(\mathbf{x}, t) = \Delta u(\mathbf{x}, t) + F(\mathbf{x}, t, u(\mathbf{x}, t), \nabla u(\mathbf{x}, t)) & (\mathbf{x}, t) \in \mathbb{R}^d \times (0, T) \\ u(\mathbf{x}, 0) = p(\mathbf{x}) & \mathbf{x} \in \mathbb{R}^d, \end{cases} \quad (1.1)$$

where  $p \in C_c^1(\mathbb{R}^d)$  is a source function. Assume that  $p$  is compactly supported in  $\Omega$ . Since the main aim of this paper concerns with inverse problem, not forward problem, the existence, uniqueness and regularity

---

\*Department of Mathematics and Statistics, University of North Carolina at Charlotte, Charlotte, NC 28223, USA, tle55@uncc.edu.

results for the solution to (1.1) are considered as assumptions. For the completeness, we provide here a set of conditions that guarantees that these assumptions hold true. Assume that  $p(\mathbf{x})$  is in  $H^{2+\beta}(\mathbb{R}^d)$  for some  $\beta \in [0, 1 + 4/d]$ . Assume further for all  $\mathbf{x} \in \mathbb{R}^d$ ,  $t \in [0, T]$ ,  $s \in \mathbb{R}$ , and  $r \in \mathbb{R}^d$ ,

$$|F(\mathbf{x}, t, s, r)| \leq C \max \{(1 + |r|)^2, 1 + |s|\}$$

for some positive constant  $C$ . Then, due to Theorem 6.1 in [21, Chapter 5, §6] and Theorem 2.1 in [21, Chapter 5, §2], problem (1.1) has a unique solution with  $|u(\mathbf{x}, t)| \leq M_1$ ,  $|\nabla u(\mathbf{x}, t)| \leq M_2$  for some positive constants  $M_1, M_2$ , and  $u(\mathbf{x}, t) \in H^{2+\beta, 1+\beta/2}(\mathbb{R}^d \times [0, T])$ .

We are interested in the problem of determining the source function  $p(\mathbf{x})$ ,  $\mathbf{x} \in \Omega$ , from the lateral Cauchy data. This problem is formulated as follows.

**Problem 1.1** (Inverse Source Problem). *Assume that  $\|u\|_{C^1(\overline{\Omega_T})} \leq M$  for some known large number  $M$ . Given the lateral Cauchy data*

$$g(\mathbf{x}, t) = u(\mathbf{x}, t) \quad \text{and} \quad q(\mathbf{x}, t) = \partial_\nu u(\mathbf{x}, t) \tag{1.2}$$

for  $\mathbf{x} \in \partial\Omega$ ,  $t \in [0, T]$ , determine the function  $u(\mathbf{x}, 0) = p(\mathbf{x})$ ,  $\mathbf{x} \in \Omega$ .

The uniqueness of Problem 1.1 is still an open question. We temporarily consider the uniqueness as an assumption. This result will be written in a separate paper. In the case when (1.1) is linear, the uniqueness of Problem 1.1 is well-known, see [23]. The logarithmic stability results in the linear case were rigorously proved in [7, 28].

A natural approach to solve the Problem 1.1 are based on least squares optimization. However, since our problem is highly nonlinear, the cost functional might have multiple minima and ravines. Thus, optimization-based methods might not deliver good solutions; especially, when a good initial guess is unavailable. An effective way to overcome the lack of a good initial guess is the convexification method, which first introduced in [10]. The main idea of the convexification method is to convexify the cost functional by employing a suitable Carleman weight function. We refer the reader to [6, 2, 38, 40, 9, 39, 11, 12, 13, 18, 19, 17, 37, 26, 15] for the development of the convexification method. Although effective, the convexification method is time consuming. Therefore, another method should be investigated.

In this paper, we introduce an iterative method to solve Problem 1.1. The first step in our numerical method is to derive a system of quasi-linear elliptic equations whose solution yields directly the solution of Problem 1.1 by truncating a Fourier series with respect to the special basis in [9]. In the second step, we propose a fixed point-like iterative process to solve the system mentioned above. The iterative process can start from an arbitrarily function. The idea to design the iterative process is similar to [25, 24, 34, 33]. Especially, in [25], we study a similar problem to recover the initial condition of a nonlinear parabolic equation from the lateral Cauchy data. The main difference between [25] and this paper is that in this paper, we study a more complicated case at which the nonlinear term  $F$  depends on both  $u(\mathbf{x}, t)$  and  $\nabla u(\mathbf{x}, t)$ . The convergence of our scheme is rigorously proved based on a Carleman estimate and the analogue contraction mapping principle. Our iterative scheme converges quickly to the true solution at the rate  $\theta^n$  for some constant  $\theta \in (0, 1)$  and  $n$  is the number of iterations. In particular, the convergence of our numerical method is rigorously proved in  $H^2$ . This result is a significant improvement in comparison to the main theorem in [30, 33] which shows a similar convergence in  $H^1$  only. These results is verified rigorously by our numerical tests.

The paper is organized as follows. In Section 2, we recall some preliminaries which we employ directly in our numerical method, including a Carleman estimate and a special orthonormal basis. In Section 3, we introduce two steps to solve Problem 1.1. The first step is to derive a system of nonlinear PDEs whose

solutions yields directly the solutions to Problem 1.1. The second step is to establish an iterative scheme to solve the above system of nonlinear PDEs. In Section 4, we prove the convergence of our iterative scheme to the true solution. In Section 5, we discuss the implementation of our method and present some numerical results. Section 6 is some concluding remarks.

## 2 Preliminaries

In this section, we recall a Carleman estimate established in [25]. This Carleman estimate plays an important role this paper. On the other hand, we recall a special orthonormal basis  $\{\Phi_n\}_{n \geq 1}$  of  $L^2(0, T)$ , which will be used in the numerical implementation section, Section 5. This special basis was first introduced in [9].

### 2.1 A Carleman estimate

The Carleman estimate is a powerful tool in the field of PDEs which were first employed to prove the unique continuation principle, see [5, 36], the uniqueness of a long list of inverse problems, see [4] and in cloaking [31]. Here we recall a Carleman estimate which was established in [25]. The analysis of this paper is based on this Carleman estimate.

**Lemma 2.1** (Carleman estimate, see [25]). *Let  $\mathbf{x}_0$  be a point in  $\mathbb{R}^d \setminus \bar{\Omega}$  such that  $r(\mathbf{x}) = |\mathbf{x} - \mathbf{x}_0| > 1$  for all  $\mathbf{x} \in \Omega$ . Let  $b > \max_{\mathbf{x} \in \bar{\Omega}} r(\mathbf{x})$  be a fixed constant. There exist positive constants  $\beta_0$  depending only on  $b, \mathbf{x}_0, \Omega$  and  $d$  such that for all function  $v \in C^2(\bar{\Omega})$  satisfying*

$$v(\mathbf{x}) = \partial_\nu v(\mathbf{x}) = 0 \quad \text{for all } \mathbf{x} \in \partial\Omega,$$

the following estimate holds true

$$\begin{aligned} \int_{\Omega} e^{2\lambda b^{-\beta} r^\beta(\mathbf{x})} |\Delta v(\mathbf{x})|^2 d\mathbf{x} &\geq \frac{C}{\lambda \beta^{7/4} b^{-\beta}} \int_{\Omega} e^{2\lambda b^{-\beta} r^\beta(\mathbf{x})} r^{2\beta}(\mathbf{x}) |D^2 v(\mathbf{x})|^2 d\mathbf{x} \\ &\quad + C \lambda^3 \beta^4 b^{-3\beta} \int_{\Omega} r^{2\beta}(\mathbf{x}) e^{2\lambda b^{-\beta} r^\beta} |v(\mathbf{x})|^2 d\mathbf{x} \\ &\quad + C \lambda \beta^{1/2} b^{-\beta} \int_{\Omega} e^{2\lambda b^{-\beta} r^\beta(\mathbf{x})} |\nabla v(\mathbf{x})|^2 d\mathbf{x} \end{aligned} \quad (2.1)$$

for  $\beta \geq \beta_0$  and  $\lambda \geq \lambda_0$ . Here,  $D^2 v = (v_{x_i x_j})_{i, j=1}^d$  is the Hessian matrix of  $v$ ,  $\lambda_0 = \lambda_0(b, \Omega, d, \mathbf{x}_0) > 1$  is a positive number with  $\lambda_0 b^{-\beta} \gg 1$  and  $C = C(b, \Omega, d, \mathbf{x}_0) > 1$  is a constant. These numbers depend only on listed parameters.

**Corollary 2.1.** *Recall  $\beta_0$  and  $\lambda_0$  as in Lemma 2.1. Fix  $\beta = \beta_0$  and let the constant  $C$  depend on  $\mathbf{x}_0, \Omega, d$  and  $\beta$ . There exists a constant  $\lambda_0$  depending only on  $\mathbf{x}_0, \Omega, d$  and  $\beta$  such that for all function  $v \in H^2(\Omega)$  with*

$$v(\mathbf{x}) = \partial_\nu v(\mathbf{x}) = 0 \quad \text{on } \partial\Omega,$$

we have

$$\begin{aligned} \int_{\Omega} e^{2\lambda b^{-\beta} r^\beta(\mathbf{x})} |\Delta v(\mathbf{x})|^2 d\mathbf{x} &\geq C \lambda^{-1} \int_{\Omega} e^{2\lambda b^{-\beta} r^\beta(\mathbf{x})} |D^2 v(\mathbf{x})|^2 d\mathbf{x} \\ &\quad + C \lambda^3 \int_{\Omega} e^{2\lambda b^{-\beta} r^\beta} |v(\mathbf{x})|^2 d\mathbf{x} + C \lambda \int_{\Omega} e^{2\lambda b^{-\beta} r^\beta(\mathbf{x})} |\nabla v(\mathbf{x})|^2 d\mathbf{x} \end{aligned} \quad (2.2)$$

for all  $\lambda \geq \lambda_0$ .

We refer the reader to [25, Theorem 3.1] for the proof of Lemma 2.1. We also refer the readers to [29, 35] for some versions of Carleman estimates for parabolic operators, and to [3, 4, 16] for several other versions of Carleman estimates for a variety kinds of differential operators and their applications in inverse problems.

## 2.2 A special orthonormal basis

In this section, we recall a special basis of  $L^2(0, T)$ . This special basis will be employed in our numerical study. Let  $\phi_n(t) = (t - T/2)^{n-1} e^{t-T/2}$  for  $n \in \mathbb{N}$ . The set  $\{\phi_n\}_{n=1}^\infty$  is complete in  $L^2(0, T)$ . Applying the GramSchmidt orthonormalization process to this complete set gives a basis of  $L^2(0, T)$ , named as  $\{\Psi_n\}_{n=1}^\infty$ . The following proposition holds true.

**Proposition 2.1** (see [9]). *The basis  $\{\Psi_n\}_{n=1}^\infty$  satisfies the following properties:*

(i)  $\Psi'_n$  is not identically zero for all  $n \geq 1$

(ii) For all  $m, n \geq 1$

$$s_{mn} = \int_0^T \Psi'_n(t) \Psi_m(t) dt = \begin{cases} 1 & \text{if } m = n, \\ 0 & \text{if } n < m. \end{cases} \quad (2.3)$$

As a results, for all integer  $N > 1$ , the matrix  $S = (s_{mn})_{m,n=1}^N$  is invertible.

This basis was first introduced to solve the electrical impedance tomography problem with partial data in [9]. Afterward, it is widely used in our research group to solve a variety kinds of inverse problems, including ill-posed inverse source problems for elliptic equations [35], parabolic equations [25] [29] and hyperbolic equations [27], nonlinear coefficient inverse problems for elliptic equations [38], and parabolic equations [20, 40, 32, 39, 26], transport equations [14] and full transfer equations [37].

## 3 A numerical method to solve Problem 1.1

In this section, we present our numerical method to solve Problem 1.1. Our method consists of two (2) main steps. Firstly, we derive a nonlinear system of elliptic equations by cutting of a Fourier series with respect to an orthonormal basis of  $L^2(0, T)$ . Solution of this system directly leads to that of Problem 1.1. Secondly, we propose a fixed point-like iterative scheme to solve the nonlinear system mentioned in step 1.

### 3.1 A system of nonlinear elliptic equations

Let  $\{\Psi_n\}_{n=1}^\infty$  be an orthonormal basis of  $L^2(0, T)$ . For all  $(\mathbf{x}, t) \in Q_T$ , we can approximate  $u(\mathbf{x}, t)$  as follows.

$$u(\mathbf{x}, t) = \sum_{n=1}^{\infty} u_n(\mathbf{x}) \Psi_n(t) \quad (3.1)$$

where

$$u_n(\mathbf{x}) = \int_0^T u(\mathbf{x}, t) \Psi_n(t) dt \quad \text{for all } n \geq 1. \quad (3.2)$$

We now derive our approximation model. For some cut-off number  $N$ , chosen later in Section 5, we approximate the function  $u(\mathbf{x}, t)$  by truncating the series in (3.1) as

$$u(\mathbf{x}, t) \approx u^N(\mathbf{x}, t) := \sum_{n=1}^N u_n(\mathbf{x})\Psi_n(t) \quad \text{for all } (\mathbf{x}, t) \in Q_T \quad (3.3)$$

We also approximate

$$u_t(\mathbf{x}, t) \approx u_t^N(\mathbf{x}, t) := \sum_{n=1}^N u_n(\mathbf{x})\Psi'_n(t) \quad \text{for all } (\mathbf{x}, t) \in Q_T \quad (3.4)$$

**Remark 3.1.** *The approximation in (3.3) is numerically verified by Figure 1.*

Plugging (3.3) and (3.4) into the governing equation (1.1), we obtain

$$c(\mathbf{x}) \sum_{n=1}^N u_n(\mathbf{x})\Psi'_n(t) = \sum_{n=1}^N \Delta u_n(\mathbf{x})\Psi_n(t) + F\left(\mathbf{x}, t, \sum_{n=1}^N u_n(\mathbf{x})\Psi_n(t), \sum_{n=1}^N \nabla u_n(\mathbf{x})\Psi_n(t)\right) \quad (3.5)$$

for all  $(\mathbf{x}, t) \in Q_T$ .

**Remark 3.2.** *The cut-off number  $N$  is chosen numerically such that  $u^N$  well approximates the function  $u$ , see Section 5.2 for more details. Due to the nonlinearity and the ill-posedness of this inverse source problem, studying the convergence of (3.5) as  $N \rightarrow \infty$  is extremely challenging and out of scope of this paper. We only solve Problem 1.1 in the approximation context.*

For each  $m \in \{1, \dots, N\}$ , multiplying  $\Psi_m(t)$  to both sides of (3.5) and then integrating the obtained equation with respect to  $t$  give

$$\begin{aligned} c(\mathbf{x}) \sum_{n=1}^N u_n(\mathbf{x}) \int_0^T \Psi'_n(t)\Psi_m(t)dt &= \sum_{n=1}^N \Delta u_n(\mathbf{x}) \int_0^T \Psi_n(t)\Psi_m(t)dt \\ &+ \int_0^T F\left(\mathbf{x}, t, \sum_{n=1}^N u_n(\mathbf{x})\Psi_n(t), \sum_{n=1}^N \nabla u_n(\mathbf{x})\Psi_n(t)\right) \Psi_m(t)dt. \end{aligned} \quad (3.6)$$

Since  $\{\Psi_n\}_{n \geq 1}$  is an orthonormal basis, system (3.6) can be rewritten as

$$c(\mathbf{x}) \sum_{n=1}^N s_{mn}u_n(\mathbf{x}) = \Delta u_m(\mathbf{x}) + F_m(\mathbf{x}, U(\mathbf{x}), \nabla U(\mathbf{x})) \quad (3.7)$$

for all  $\mathbf{x} \in \Omega$  and  $m = 1, \dots, N$  where  $U = (u_1, u_2, \dots, u_N)^T$ ,

$$s_{mn} = \int_0^T \Psi'_n(t)\Psi_m(t)dt$$

and

$$F_m(\mathbf{x}, U(\mathbf{x}), \nabla U(\mathbf{x})) = \int_0^T F\left(\mathbf{x}, t, \sum_{n=1}^N u_n(\mathbf{x})\Psi_n(t), \sum_{n=1}^N \nabla u_n(\mathbf{x})\Psi_n(t)\right) \Psi_m(t)dt.$$

Denote by  $S$  the matrix  $(s_{mn})_{m,n=1}^N$  and  $\mathbf{F} = (F_1, F_2, \dots, F_N)^T$ . We can rewrite (3.7) as

$$\Delta U(\mathbf{x}) - c(\mathbf{x})SU(\mathbf{x}) + \mathbf{F}(\mathbf{x}, U(\mathbf{x}), \nabla U(\mathbf{x})) = 0 \quad \text{for all } \mathbf{x} \in \Omega. \quad (3.8)$$

We next compute the Cauchy boundary conditions for  $U_N$ . Due to (3.2),

$$\begin{cases} U(\mathbf{x}) = G(\mathbf{x}) = \left( \int_0^T g(\mathbf{x}, t) \Psi_m(t) dt \right)_{m=1}^N, \\ \partial_\nu U(\mathbf{x}) = Q(\mathbf{x}) = \left( \int_0^T q(\mathbf{x}, t) \Psi_m(t) dt \right)_{m=1}^N \end{cases} \quad m = 1, 2, \dots, N \quad (3.9)$$

for all  $\mathbf{x} \in \partial\Omega$ ,  $m = 1, \dots, N$ , where  $g(\mathbf{x}, t)$  and  $q(\mathbf{x}, t)$  are the given data in Problem 1.1.

Combining (3.8) and (3.9), we obtain the system of elliptic equations for  $u_m(\mathbf{x})$  for each  $m = 1, \dots, N$

$$\begin{cases} \Delta U(\mathbf{x}) - c(\mathbf{x})SU(\mathbf{x}) + \mathbf{F}(\mathbf{x}, U(\mathbf{x}), \nabla U(\mathbf{x})) = 0 & \mathbf{x} \in \Omega, \\ U(\mathbf{x}) = G(\mathbf{x}) & \mathbf{x} \in \partial\Omega, \\ \partial_\nu U(\mathbf{x}) = Q(\mathbf{x}) & \mathbf{x} \in \partial\Omega. \end{cases} \quad (3.10)$$

**Remark 3.3.** *Due to the truncation in (3.3), Problem (3.10) is not exact. It is an approximation model. Proving the convergence of this approximation model as  $N \rightarrow \infty$  is extremely challenging. Establishing this result is out of the scope of this paper. The accuracy of (3.3) can be verified numerically, see Figure 1.*

Problem 1.1 is reduced to the problem of finding  $U = (u_1, u_2, \dots, u_N)^T$  satisfying system (3.10). In fact, if this vector is known, the function  $u(\mathbf{x}, t)$  for all  $(\mathbf{x}, t) \in Q_T$  can be approximated via (3.3). Then, the solution to Problem 1.1 is given by  $p(\mathbf{x}) = u(\mathbf{x}, 0)$  for all  $\mathbf{x} \in \Omega$ . In the next section, we introduce an iterative procedure to solve system (3.10).

### 3.2 An iterative procedure to solve system (3.10)

We introduce an iterative scheme to solve system (3.10). The convergence of this scheme to the true solution of (3.10) will be discussed later in Section 4.

Let  $U^{(0)}$  be an arbitrary vector-valued function. Assume by induction that we know  $U^{(k-1)}$  for  $k \geq 1$ . We then find  $U^{(k)}$  by solving the following system

$$\begin{cases} \Delta U^{(k)}(\mathbf{x}) - c(\mathbf{x})SU^{(k)}(\mathbf{x}) = -\mathbf{F}(\mathbf{x}, U^{(k-1)}(\mathbf{x}), \nabla U^{(k-1)}(\mathbf{x})) & \mathbf{x} \in \Omega, \\ U^{(k)}(\mathbf{x}) = G(\mathbf{x}) & \mathbf{x} \in \partial\Omega, \\ \partial_\nu U^{(k)}(\mathbf{x}) = Q(\mathbf{x}) & \mathbf{x} \in \partial\Omega. \end{cases} \quad (3.11)$$

Problem (3.11) might not have a solution because it is over-determined. We only compute the ‘‘Carleman best-fit’’ solution  $U^{(k)}$  to (3.11) by combining the quasi-reversibility method and a Carleman weight function as follows. The convergence of the sequence of ‘‘Carleman best-fit’’ solutions is one of the important strengths of this paper. Define the set of admissible solutions

$$H = \{V \in H^2(\Omega)^N : V|_{\partial\Omega} = G \text{ and } \partial_\nu V|_{\partial\Omega} = Q\}. \quad (3.12)$$

Throughout this paper, we assume that  $H$  is nonempty. Recall  $\beta_0$  and  $\lambda_0$  as in Lemma 2.1. Fix  $\beta > \beta_0$ . For each  $\lambda > \lambda_0$ , we define the following Carleman weighted least squares functional

$$J^{(k)}(V) = \int_{\Omega} e^{2\lambda b^{-\beta} r^\beta(\mathbf{x})} \left| \Delta V - c(\mathbf{x})SV + \mathbf{F}(\mathbf{x}, U^{(k-1)}, \nabla U^{(k-1)}) \right|^2 d\mathbf{x} \quad (3.13)$$

for  $V \in H$ . Then, we set

$$U^{(k)} = \operatorname{argmin}_{V \in H} J^{(k)}(V). \quad (3.14)$$

See Theorem 4.1 for the existence and uniqueness of the minimizer of  $J^{(k)}$ .

Recall that the function  $U^{(k)}$  is called the ‘‘Carleman best fit’’ solution to (3.11) obtained by the Carleman quasi-reversibility method. The original quasi-reversibility method was introduced by Lattès and Lions in 1969, see [22]. We refer readers to [29, 35, 27] for using the quasi-reversibility method to solve a linear system of PDEs and [8] for a survey of the quasi-reversibility method. In the original quasi-reversibility method, the best fit solutions to (3.11) can be found by minimizing the least-squares functional. Here, we improve this method by imposing a Carleman weight function on the original least-squares functional. By ‘‘improve’’, we mean that the presence of the Carleman weight function plays a crucial role in the convergence analysis in the next section. More precisely, we will show that the sequence  $\{U^{(k)}\}_{k \geq 0}$  converges to the true solution to (3.10) as  $k$  goes to  $\infty$ . The choice of the initial term does not matter.

We summary the procedure to solve Problem 1.1 in the Algorithm.

---

**Algorithm 1** The procedure to solve Problem 1.1

---

- 1: Choose an orthonormal basis  $(\Psi_n)_{n \geq 1}$  and a cut-off number  $N$ .
- 2: Compute the Cauchy data  $G$  and  $Q$  on  $\partial\Omega$  as in (3.9).
- 3: Choose an arbitrary vector valued function  $U^{(0)} \in H^2(\Omega)^N$ .
- 4: By induction, we assume that we known  $U^{(k-1)}$   $k \geq 1$ . Solve the system (3.11) by Carleman quasi-reversibility method for the vector valued function  $U^{(k)} = \left(u_1^{(k)}, \dots, u_m^{(k)}\right)^T$ .
- 5: Set the computed source function at step  $k$  is

$$p^{(k)}(\mathbf{x}) = u^{(k)}(\mathbf{x}, 0) = \sum_{n=1}^N u_n^{(k)}(\mathbf{x}) \Psi_n(0)$$

- 6: Set the computed source function is  $p_{\text{comp}} = p^{(k)}$  for  $k = \bar{k}$  large enough.
- 

## 4 The main theorems

We establish two theorems in this section. The first one proves that the sequence  $\{U_N^{(k)}\}_{k \geq 0}$ , constructed in Section 3.2 and (3.14), is well-defined. The second one guarantees the convergence of  $\{U_N^{(k)}\}_{k \geq 0}$ .

**Theorem 4.1.** *Fix  $\beta = \beta_0$  and choose  $\lambda > \lambda_0$ , where  $\beta_0$  and  $\lambda_0$  are in Lemma 2.1 and Corollary 2.1, such that (2.2) holds true. For each  $k \geq 1$ , the functional  $J^{(k)}$ , defined in (3.13), has a unique minimizer in  $H$ .*

*Proof.* The proof of Theorem 4.1 is based on the Riesz Representation Theorem. Since the set of admissible solutions  $H$  is nonempty, we can find a vector valued function  $\Phi = (\phi_1, \dots, \phi_N)^T$  in  $H$ . Define

$$H_0 = \{U - \Phi \in H^2(\Omega)^N : U \in H\} \quad (4.1)$$

It is obvious that for all  $V = (v_1, \dots, v_N)^T \in H_0$ ,  $V|_{\partial\Omega} = 0$  and  $\partial_\nu V|_{\partial\Omega} = 0$ . Using the trace theory, we can see that  $H_0$  is a closed subspace of  $H^2(\Omega)^N$ .

Define the bounded bilinear form  $a : H_0 \times H_0 \rightarrow \mathbb{R}$  and the bounded linear map  $L : H_0 \rightarrow \mathbb{R}$  as

$$a(P, Q) = \int_{\Omega} e^{2\lambda b^{-\beta} r^{\beta}(\mathbf{x})} (\Delta P - c(\mathbf{x})SP) \cdot (\Delta Q - c(\mathbf{x})SQ) d\mathbf{x}$$

and

$$LQ = - \int_{\Omega} e^{2\lambda b^{-\beta} r^{\beta}(\mathbf{x})} (\Delta \Phi(\mathbf{x}) - c(\mathbf{x})S\Phi + \mathbf{F}(\mathbf{x}, U^{(k-1)}, \nabla U^{(k-1)})) \cdot (\Delta Q(\mathbf{x}) - c(\mathbf{x})SQ) d\mathbf{x} \quad (4.2)$$

for all  $P, Q \in H_0$ .

We will show that  $a(P, Q)$  is an inner product on  $H_0$  and equivalent to the standard norm in  $H^2(\Omega)^N$ . In fact, for all  $P \in H_0$ ,

$$a(P, P) = \int_{\Omega} e^{2\lambda b^{-\beta} r^{\beta}(\mathbf{x})} |\Delta P - c(\mathbf{x})SP|^2 d\mathbf{x} \leq C \|P\|_{H^2(\Omega)^N}^2. \quad (4.3)$$

On the other hand, for all  $P \in H_0$ , using the inequality  $(x - y)^2 \geq \frac{1}{2}x^2 - y^2$ , we have

$$\begin{aligned} a(P, P) &= \int_{\Omega} e^{2\lambda b^{-\beta} r^{\beta}(\mathbf{x})} |\Delta P - c(\mathbf{x})SP|^2 d\mathbf{x} \\ &\geq \frac{1}{2} \int_{\Omega} e^{2\lambda b^{-\beta} r^{\beta}(\mathbf{x})} |\Delta P|^2 d\mathbf{x} - \int_{\Omega} e^{2\lambda b^{-\beta} r^{\beta}(\mathbf{x})} |c(\mathbf{x})SP|^2 d\mathbf{x}. \end{aligned} \quad (4.4)$$

Applying the Carleman estimate (2.2) for vector  $P \in H_0$ , we have

$$\begin{aligned} a(P, P) &\geq C\lambda^{-1} \int_{\Omega} e^{2\lambda b^{-\beta} r^{\beta}(\mathbf{x})} |D^2 P|^2 d\mathbf{x} \\ &\quad + C\lambda^3 \int_{\Omega} e^{2\lambda b^{-\beta} r^{\beta}(\mathbf{x})} |P|^2 d\mathbf{x} + C\lambda \int_{\Omega} e^{2\lambda b^{-\beta} r^{\beta}(\mathbf{x})} |\nabla P|^2 d\mathbf{x} \\ &\quad - \int_{\Omega} e^{2\lambda b^{-\beta} r^{\beta}(\mathbf{x})} |c(\mathbf{x})SP|^2 d\mathbf{x}. \end{aligned} \quad (4.5)$$

This estimate leads to

$$a(P, P) \geq C \|P\|_{H^2(\Omega)^N}^2. \quad (4.6)$$

Hence, due to (4.3) and (4.6), the bilinear form  $a$  defines an inner product on  $H_0$ , denoted by  $a(\cdot, \cdot)$ . This new inner product is equivalent to the traditional one of  $H^2(\Omega)^N$ .

Recall that  $L$  is a bounded linear map. Using the Riesz Representation Theorem for  $H_0$  with the inner product  $a(\cdot, \cdot)$ , there exists a unique vector  $W_0$  such that

$$a(W_0, Q) = LQ \text{ for all } Q \in H_0 \quad (4.7)$$

This means

$$\begin{aligned} &\int_{\Omega} e^{2\lambda b^{-\beta} r^{\beta}(\mathbf{x})} (\Delta W_0 - c(\mathbf{x})SW_0) (\Delta Q - c(\mathbf{x})SQ) d\mathbf{x} \\ &= - \int_{\Omega} e^{2\lambda b^{-\beta} r^{\beta}(\mathbf{x})} (\Delta \Phi - c(\mathbf{x})S\Phi + \mathbf{F}(\mathbf{x}, U^{(k-1)}, \nabla U^{(k-1)})) \cdot (\Delta Q - c(\mathbf{x})SQ) d\mathbf{x} \end{aligned} \quad (4.8)$$



for all  $Q \in H_0$ . It implies that

$$\int_{\Omega} e^{2\lambda b^{-\beta} r^{\beta}(\mathbf{x})} (\Delta W_0 - c(\mathbf{x})S W_0 + \Delta \Phi - c(\mathbf{x})S \Phi + \mathbf{F}(\mathbf{x}, U^{(k-1)}, \nabla U^{(k-1)})) \cdot (\Delta Q - c(\mathbf{x})S Q) d\mathbf{x} = 0 \quad (4.9)$$

for all  $Q \in H_0$ .

Let  $U_0 = W_0 + \Phi \in H$ . It follows from (4.9) that

$$\int_{\Omega} e^{2\lambda b^{-\beta} r^{\beta}(\mathbf{x})} (\Delta U_0 - c(\mathbf{x})S U_0 + \mathbf{F}(\mathbf{x}, U^{(k-1)}, \nabla U^{(k-1)})) \cdot (\Delta Q - c(\mathbf{x})S Q) d\mathbf{x} = 0 \quad (4.10)$$

for all  $Q \in H_0$ . We next claim that  $U_0$  is a minimizer of the functional  $J^{(k)}$  defined in (3.13). In fact, for all  $U \in H$ , define  $h = U - U_0 \in H_0$ , we have

$$\begin{aligned} J^{(k)}(U) - J^{(k)}(U_0) &= J^{(k)}(U_0 + h) - J^{(k)}(U_0) \\ &= \int_{\Omega} e^{2\lambda b^{-\beta} r^{\beta}(\mathbf{x})} \left| \Delta(U_0 + h) - c(\mathbf{x})S(U_0 + h) + \mathbf{F}(\mathbf{x}, U^{(k-1)}, \nabla U^{(k-1)}) \right|^2 d\mathbf{x} \\ &\quad - \int_{\Omega} e^{2\lambda b^{-\beta} r^{\beta}(\mathbf{x})} \left| \Delta U_0 - c(\mathbf{x})S U_0 + \mathbf{F}(\mathbf{x}, U^{(k-1)}, \nabla U^{(k-1)}) \right|^2 d\mathbf{x} \end{aligned}$$

Applying  $(a + b)^2 = a^2 + 2ab + b^2$ , we have

$$\begin{aligned} J^{(k)}(U) - J^{(k)}(U_0) &= \int_{\Omega} e^{2\lambda b^{-\beta} r^{\beta}(\mathbf{x})} |\Delta h - c(\mathbf{x})S h|^2 d\mathbf{x} \\ &\quad + 2 \int_{\Omega} e^{2\lambda b^{-\beta} r^{\beta}(\mathbf{x})} \left( \Delta U_0 - c(\mathbf{x})S U_0 + \mathbf{F}(\mathbf{x}, U^{(k-1)}, \nabla U^{(k-1)}) \right) (\Delta h - c(\mathbf{x})S h) d\mathbf{x} \end{aligned} \quad (4.11)$$

It follows from (4.10) and (4.11) that

$$J^{(k)}(U) - J^{(k)}(U_0) = \int_{\Omega} e^{2\lambda b^{-\beta} r^{\beta}(\mathbf{x})} |\Delta h - c(\mathbf{x})S h|^2 d\mathbf{x} \geq 0$$

for all  $U \in H$ . As a result,  $U_0$  is a minimizer of  $J^{(k)}$  in  $H$ . The uniqueness of the minimizer is due to the strict convexity of  $J^{(k)}$  in  $H$ .  $\square$

We next rigorously prove that the sequence of vectors,  $\{U^{(k)}\}_{k \geq 1}$ , defined in (3.14) in Section 3.2, converges to the true solution to 3.10. We first consider the simple case when  $\|F\|_{C^1(\mathbb{R}, \mathbb{R}^d)} < \infty$ . The case when  $\|F\|_{C^1(\mathbb{R}, \mathbb{R}^d)} = \infty$  will follow by using a truncation technique, see Remark 4.3.

**Theorem 4.2.** *Let  $\beta_0$  be as in Lemma 2.1. Fix  $\beta = \beta_0$  and let  $\lambda_0$  be the number as in Lemma 2.1 depending only on  $\mathbf{x}_0$ ,  $\Omega$ ,  $d$  and  $\beta$ . For all  $\lambda \geq \lambda_0$ , define the sequence  $\{U^{(k)}\}_{k \geq 0}$  as in (3.14) in Section 3.2 where  $U^{(0)}$  is an arbitrary function in  $H^2(\Omega)^N$ . Assume that  $\|F\|_{C^1(\mathbb{R}, \mathbb{R}^d)} < \infty$ . Assume further that the system (3.10) has a unique solution  $U^*$ . Then, we have*

$$\begin{aligned} &\int_{\Omega} e^{2\lambda b^{-\beta} r^{\beta}(\mathbf{x})} \left( \lambda^{-2} |D^2(U^{(k)} - U^*)|^2 + |\nabla(U^{(k)} - U^*)|^2 + |U^{(k)} - U^*|^2 \right) d\mathbf{x} \\ &\leq \left( \frac{C}{\lambda} \right)^k \int_{\Omega} e^{2\lambda b^{-\beta} r^{\beta}(\mathbf{x})} \left( \lambda^{-2} |D^2(U^{(0)} - U^*)|^2 + |\nabla(U^{(0)} - U^*)|^2 + |U^{(0)} - U^*|^2 \right), \end{aligned} \quad (4.12)$$

for  $k = 1, 2, \dots$  where  $C$  is a constant depending only on  $\mathbf{x}_0$ ,  $\Omega$ ,  $d$ , and  $\|F\|_{C^1(\mathbb{R}, \mathbb{R}^d)}$ .

*Proof.* In this proof,  $C$  denotes different positive constants that might change from estimate to estimate. Define

$$H_0 = \{V \in H^2(\Omega)^N : V|_{\partial\Omega} = 0 \text{ and } \partial_\nu V|_{\partial\Omega} = 0\}. \quad (4.13)$$

It is obvious  $H_0$  a closed subspace of  $H^2(\Omega)^N$ . Since  $U^{(k)}$  is the minimizer of  $J^{(k)}$  in  $H$ , by the variational principle, the following identity holds

$$\left\langle e^{\lambda b^{-\beta} r^\beta(\mathbf{x})} \left[ \Delta U^{(k)} - c(\mathbf{x}) S U^{(k)} + \mathbf{F}(\mathbf{x}, U^{(k-1)}, \nabla U^{(k-1)}) \right], e^{\lambda b^{-\beta} r^\beta(\mathbf{x})} \left[ \Delta h(\mathbf{x}) - c(\mathbf{x}) S h \right] \right\rangle_{L^2(\Omega)^N} = 0 \quad (4.14)$$

for all  $h \in H_0$ . On the other hand, since  $U^*$  is the solution to system (3.10),

$$\left\langle e^{\lambda b^{-\beta} r^\beta(\mathbf{x})} \left[ \Delta U^* - c(\mathbf{x}) S U^* + \mathbf{F}(\mathbf{x}, U^*, \nabla U^*) \right], e^{\lambda b^{-\beta} r^\beta(\mathbf{x})} \left[ \Delta h - c(\mathbf{x}) S h \right] \right\rangle_{L^2(\Omega)^N} = 0 \quad (4.15)$$

for all  $h \in H_0$ . Subtracting (4.15) from (4.14), we obtain

$$\left\langle e^{\lambda b^{-\beta} r^\beta(\mathbf{x})} \left[ \Delta(U^{(k)} - U^*) - c(\mathbf{x}) S(U^{(k)} - U^*) + \mathbf{F}(\mathbf{x}, U^{(k-1)}, \nabla U^{(k-1)}) - \mathbf{F}(\mathbf{x}, U^*, \nabla U^*) \right], e^{\lambda b^{-\beta} r^\beta(\mathbf{x})} \left[ \Delta h - c(\mathbf{x}) S h \right] \right\rangle_{L^2(\Omega)^N} = 0 \quad (4.16)$$

for all  $h \in H_0$ . Using the test function  $h = U^{(k)} - U^* \in H_0$  and Hölder's inequality, we obtain from identity (4.16) that

$$\begin{aligned} & \int_{\Omega} e^{2\lambda b^{-\beta} r^\beta(\mathbf{x})} |\Delta h - c(\mathbf{x}) S h|^2 d\mathbf{x} \\ & \leq \left[ \int_{\Omega} e^{2\lambda b^{-\beta} r^\beta(\mathbf{x})} |\mathbf{F}(\mathbf{x}, U^{(k-1)}, \nabla U^{(k-1)}) - \mathbf{F}(\mathbf{x}, U^*, \nabla U^*)|^2 d\mathbf{x} \right]^{1/2} \\ & \quad \times \left[ \int_{\Omega} e^{2\lambda b^{-\beta} r^\beta(\mathbf{x})} |\Delta h - c(\mathbf{x}) S h|^2 d\mathbf{x} \right]^{1/2}, \end{aligned} \quad (4.17)$$

which implies

$$\int_{\Omega} e^{2\lambda b^{-\beta} r^\beta(\mathbf{x})} |\Delta h - c(\mathbf{x}) S h|^2 d\mathbf{x} \leq \int_{\Omega} e^{2\lambda b^{-\beta} r^\beta(\mathbf{x})} |\mathbf{F}(\mathbf{x}, U^{(k-1)}, \nabla U^{(k-1)}) - \mathbf{F}(\mathbf{x}, U^*, \nabla U^*)|^2 d\mathbf{x}. \quad (4.18)$$

Since  $F$  has a finite  $C^1$  norm, so does  $\mathbf{F}$ . Using the inequality  $(a+b)^2 \leq 2(a^2+b^2)$ , we obtain from (4.18) that

$$\int_{\Omega} e^{2\lambda b^{-\beta} r^\beta(\mathbf{x})} |\Delta h - c(\mathbf{x}) S h|^2 d\mathbf{x} \leq C \int_{\Omega} e^{2\lambda b^{-\beta} r^\beta(\mathbf{x})} [|U^{(k-1)} - U^*|^2 + |\nabla(U^{(k-1)} - U^*)|^2] d\mathbf{x}. \quad (4.19)$$

On the other hand, applying the inequality  $(a-b)^2 \geq \frac{1}{2}a^2 - b^2$ , we get

$$\int_{\Omega} e^{2\lambda b^{-\beta} r^\beta(\mathbf{x})} |\Delta h - c(\mathbf{x}) S h|^2 d\mathbf{x} \geq \frac{1}{2} \int_{\Omega} e^{2\lambda b^{-\beta} r^\beta(\mathbf{x})} |\Delta h|^2 d\mathbf{x} - \int_{\Omega} e^{2\lambda b^{-\beta} r^\beta(\mathbf{x})} |c(\mathbf{x}) S h|^2 d\mathbf{x}. \quad (4.20)$$

Using the Carleman estimate (2.2) for the function  $h \in H_0$ , we have

$$\begin{aligned} \int_{\Omega} e^{2\lambda b^{-\beta} r^{\beta}(\mathbf{x})} |\Delta h|^2 d\mathbf{x} &\geq C\lambda^{-1} \int_{\Omega} e^{2\lambda b^{-\beta} r^{\beta}(\mathbf{x})} |D^2 h|^2 d\mathbf{x} \\ &\quad + C\lambda^3 \int_{\Omega} e^{2\lambda b^{-\beta} r^{\beta}(\mathbf{x})} |h|^2 d\mathbf{x} + C\lambda \int_{\Omega} e^{2\lambda b^{-\beta} r^{\beta}(\mathbf{x})} |\nabla h|^2 d\mathbf{x}. \end{aligned} \quad (4.21)$$

Combining (4.19), (4.20) and (4.21), we obtain

$$\begin{aligned} \lambda^{-1} \int_{\Omega} e^{2\lambda b^{-\beta} r^{\beta}(\mathbf{x})} |D^2 h|^2 d\mathbf{x} + \lambda \int_{\Omega} e^{2\lambda b^{-\beta} r^{\beta}(\mathbf{x})} (|h|^2 + |\nabla h|^2) d\mathbf{x} \\ \leq C \int_{\Omega} e^{2\lambda b^{-\beta} r^{\beta}(\mathbf{x})} (|U^{(k-1)} - U^*|^2 + |\nabla (U^{(k-1)} - U^*)|^2) d\mathbf{x}. \end{aligned} \quad (4.22)$$

Multiply both sides of (4.22) with  $\frac{1}{\lambda}$  and recall  $h = U^{(k)} - U^*$ . We have

$$\begin{aligned} \int_{\Omega} e^{2\lambda b^{-\beta} r^{\beta}(\mathbf{x})} (\lambda^{-2} |D^2 (U^{(k)} - U^*)|^2 + |\nabla (U^{(k)} - U^*)|^2 + |U^{(k)} - U^*|^2) d\mathbf{x} \\ \leq \frac{C}{\lambda} \int_{\Omega} e^{2\lambda b^{-\beta} r^{\beta}(\mathbf{x})} (|\nabla (U^{(k-1)} - U^*)|^2 + |U^{(k-1)} - U^*|^2) d\mathbf{x}, \end{aligned} \quad (4.23)$$

which implies

$$\begin{aligned} \int_{\Omega} e^{2\lambda b^{-\beta} r^{\beta}(\mathbf{x})} (\lambda^{-2} |D^2 (U^{(k)} - U^*)|^2 + |\nabla (U^{(k)} - U^*)|^2 + |U^{(k)} - U^*|^2) d\mathbf{x} \\ \leq \frac{C}{\lambda} \int_{\Omega} e^{2\lambda b^{-\beta} r^{\beta}(\mathbf{x})} (\lambda^{-2} |D^2 (U^{(k-1)} - U^*)|^2 + |\nabla (U^{(k-1)} - U^*)|^2 + |U^{(k-1)} - U^*|^2) d\mathbf{x} \end{aligned} \quad (4.24)$$

By induction, from (4.24), we have (4.12).  $\square$

**Corollary 4.1.** Fix  $\lambda$  large enough such that  $\theta = C/\lambda \in (0, 1)$  where  $C$  is the constant in (4.12). Then,

$$\begin{aligned} \min_{\mathbf{x} \in \bar{\Omega}} \{e^{2\lambda b^{-\beta} r^{\beta}(\mathbf{x})}\} \int_{\Omega} (\lambda^{-2} |D^2 (U^{(k)} - U^*)|^2 + |\nabla (U^{(k)} - U^*)|^2 + |U^{(k)} - U^*|^2) d\mathbf{x} \\ \leq \theta^k \max_{\mathbf{x} \in \bar{\Omega}} \{e^{2\lambda b^{-\beta} r^{\beta}(\mathbf{x})}\} \int_{\Omega} (\lambda^{-2} |D^2 (U^{(0)} - U^*)|^2 + |\nabla (U^{(0)} - U^*)|^2 + |U^{(0)} - U^*|^2) d\mathbf{x} \end{aligned} \quad (4.25)$$

Inequality (4.25) rigorously guarantees that the sequence  $\{U^{(k)}\}_{k \geq 1}$  converges to  $U^*$  in  $H^2(\Omega)^N$ . As a result, the sequence  $\{p^{(k)}(\mathbf{x})\}_{k \geq 1}$  obtained in Step 5 of Algorithm 1 converges to the true source function  $p^*(\mathbf{x})$  in  $H^2(\Omega)^N$  where

$$p^*(\mathbf{x}) = \sum_{n=1}^N u_n^*(\mathbf{x}) \Psi_n(0) \quad \text{for all } \mathbf{x} \in \Omega.$$

**Remark 4.1.** One of our contributions in this paper is that we rigorously prove the convergence of the iterative scheme to the true solution of the nonlinear PDEs in  $H^2(\Omega)^N$ . It is an important improvement in comparison with the main theorem in [30, 33] which prove the convergence in  $H^1$  only.

**Remark 4.2.** With the term  $\theta \in (0, 1)$ , estimate (4.25) is similar to the one in the contraction mapping principle. This explains the title of the paper.

**Remark 4.3.** In Theorem 4.2, we assume that the function  $F$  has a finite  $C^1$  norm. However, in reality,  $\|F\|_{C^1}$  might be infinity. We can extend Theorem 4.2 for the case when  $\|F\|_{C^1} = \infty$ . Recall from the statement of Problem 1.1 that  $\|u^*\|_{C^1(\overline{\Omega_T})} < M$  for some known large number  $M$ . Combining with (3.2) and noting that  $\|\Psi_n\|_{L^2(0,T)} = 1$ , we have  $\|u_m^*(\mathbf{x})\|_{C^1(\overline{\Omega})} \leq M\sqrt{T}$ . Define the smooth function  $\chi \in C^\infty(\mathbb{R} \times \mathbb{R}^d)$  as follows

$$\chi(s, \mathbf{p}) = \begin{cases} 1 & \text{if } |s| + |\mathbf{p}| < M\sqrt{T}, \\ \in (0, 1) & \text{if } M\sqrt{T} \leq |s| + |\mathbf{p}| \leq 2M\sqrt{T}, \\ 0 & \text{if } |s| + |\mathbf{p}| > 2M\sqrt{T}. \end{cases} \quad (4.26)$$

We then set  $\tilde{\mathbf{F}} = \chi\mathbf{F}$ . Since  $|u_m^*| + |\nabla u_m^*| < M$ , the vector  $U^*$  solves the following problem

$$\begin{cases} \Delta U(\mathbf{x}) - c(\mathbf{x})SU(\mathbf{x}) + \tilde{\mathbf{F}}(\mathbf{x}, U(\mathbf{x}), \nabla U(\mathbf{x})) = 0 & \mathbf{x} \in \Omega, \\ U(\mathbf{x}) = G(\mathbf{x}) & \mathbf{x} \in \partial\Omega, \\ \partial_\nu U(\mathbf{x}) = Q(\mathbf{x}) & \mathbf{x} \in \partial\Omega. \end{cases} \quad (4.27)$$

Thus, we can apply Algorithm 1 for (4.27) to compute  $U^*(\mathbf{x})$  and the source function  $p(\mathbf{x})$ .

## 5 Numerical study

In this section, we perform some numerical results obtained by Algorithm 1. For simplicity purpose, we test our method in the 2-D case, i.e.  $d=2$ .

### 5.1 The forward problem

In order to generated computationally simulated data (1.2), we need to solve numerically the forward problem. Let  $\tilde{R} > R > 0$  be two positive numbers. We define the domains

$$\tilde{\Omega} = (-\tilde{R}, \tilde{R})^2 \quad \text{and} \quad \Omega = (-R, R)^2.$$

We first solving the following problem defined in the bigger domain  $\tilde{\Omega} \times (0, T)$

$$\begin{cases} c(\mathbf{x})u_t(\mathbf{x}, t) = \Delta u(\mathbf{x}, t) + F(\mathbf{x}, t, u(\mathbf{x}, t), \nabla u(\mathbf{x}, t)) & \mathbf{x} \in \tilde{\Omega}, t \in (0, T) \\ u(\mathbf{x}, 0) = p(\mathbf{x}) & \mathbf{x} \in \tilde{\Omega}, \\ u(\mathbf{x}, t) = 0 & \mathbf{x} \in \partial\tilde{\Omega}, t \in [0, T]. \end{cases} \quad (5.1)$$

Let  $\mathbf{x} = (x, y) \in \tilde{\Omega}$ . In our numerical tests, the known coefficient function  $c(x, y)$  is set as

$$c(x, y) = 1 + \frac{1}{50} \left( 3(1-x)^2 e^{-x^2-(y+1)^2} - 10 \left( \frac{x}{5} - x^3 - y^5 \right) e^{-x^2-y^2} - \frac{1}{3} e^{-(x+1)^2-y^2} \right). \quad (5.2)$$

This function is a scale of the "peaks" function in Matlab. The values of coefficient function  $c(x, y)$  vary in the range of  $[0.8693, 1.1618]$ . We solve (5.1) by the finite difference method using the explicit scheme. Afterward, we extract the data on the boundary of the domain  $\Omega$  for the simulated data:

$$g(\mathbf{x}, t) = u(\mathbf{x}, t) \text{ and } q(\mathbf{x}, t) = \partial_\nu u(\mathbf{x}, t) \text{ for } \mathbf{x} \in \partial\Omega, t \in [0, T]$$

## 5.2 Implementation

On the domain  $\bar{\Omega}$ , we arrange an  $N_{\mathbf{x}} \times N_{\mathbf{x}}$  uniform grid

$$\mathcal{G} = \left\{ (x_i, y_j) : x_i = -R + (i-1)h, y_j = -R + (j-1)h, 1 \leq i, j \leq N_{\mathbf{x}} \right\}$$

where  $N_{\mathbf{x}}$  is the number of grid points,  $h = \frac{2R}{N_{\mathbf{x}} - 1}$  is the mesh spacing.

**Remark 5.1.** In our computations, we set  $R_1 = 6$ ,  $R = 1$ ,  $T = 1.5$ ,  $N_{\mathbf{x}} = 80$ .

In the following, we present the implementation of Algorithm 1 to solve Problem 1.1 .

**Step 1.** We employ the orthonormal basis  $\{\Psi_n\}_{n \geq 1}$  as in (2.2). The cut-off number  $N$  in our approximation of  $u(\mathbf{x}, t)$  in (3.3) is chosen as follows. We first choose a test (Test 1 in Section 5.3) as a reference test. Then, for each  $N \geq 1$ , we compute the error function

$$e_N(\mathbf{x}) = \left| u^*(\mathbf{x}, 0) - \sum_{n=1}^N u_n^*(\mathbf{x}) \Psi_n(0) \right| \quad \mathbf{x} \in \Omega \quad (5.3)$$

and choose  $N$  such that  $\|e_N\|_{L^\infty(\Omega)}$  is small enough. Figure 1 presents the values of the error  $e_N$  when  $N = 15, 35$  and  $40$ . It is obvious that increasing the value of  $N$  reduces the error. With  $N = 40$ , the error is small enough. We, therefore, choose  $N = 40$  for all numerical tests.

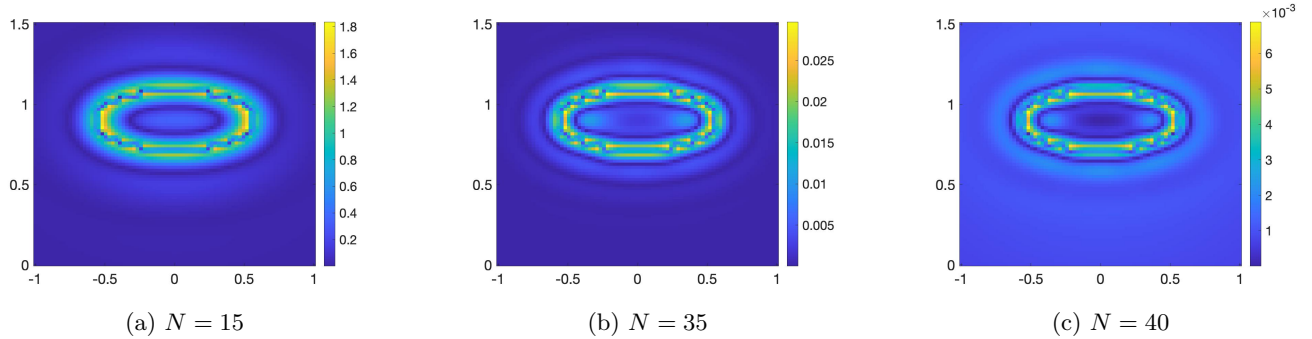


Figure 1: The function  $e_N$  defined in (5.3) where  $u^*(\mathbf{x}, 0) = p(\mathbf{x})$  is the source given in Test 1. It is evident that the larger  $N$ , the better approximation in (3.3).

**Remark 5.2.** The basis  $\{\Psi_n\}_{n \geq 1}$  in (2.2) was successfully used frequently in our research group. The reason for us to employ this basis rather than the well-known traditional “sine and cosine” basis of the Fourier series is that the first elements of the latter basis is a constant. Thus,  $u_1(\mathbf{x})\Psi_1'(t)$  vanishes. Hence, we might lose some information of  $u_1(\mathbf{x})$  in when plugging (3.4) into (1.1). This leads to a significant error in computation because the first term in the series  $\sum_{n=1}^{\infty} u_n(\mathbf{x})\Psi_n(t)$  is the most important one.

**Step 2.** We compute the “indirect data”  $G(\mathbf{x})$  and  $Q(\mathbf{x})$  on  $\partial\Omega$  as in (3.9). Denote  $G^*(\mathbf{x})$  and  $Q^*(\mathbf{x})$  as the noiseless data. The noisy data is set as follows, for  $\mathbf{x} \in \partial\Omega$

$$G^\delta(\mathbf{x}) = G^*(\mathbf{x}) (1 + \delta \text{rand}), \quad Q^\delta(\mathbf{x}) = Q^*(\mathbf{x}) (1 + \delta \text{rand})$$

for all  $\mathbf{x} \in \partial\Omega$ , where  $\delta > 0$  represents for the noise level and “rand” is the function taking uniformly distributed random numbers in the range  $[-1, 1]$ . In our numerical tests, a significant noise with noise level  $\delta = 20\%$  is involved in the data.

**Step 3.** For simplicity, we choose the initial solution  $U^{(0)} = \vec{0}$ .

**Step 4.** Given  $U^{(k-1)}$  for  $k \geq 1$ , we minimize the functional  $J^{(k)}$ , defined in (3.13), by the optimization package of MATLAB with the command “lsqin”. The implementation for the quasi-reversibility method to minimize similar functionals was described in [25, §5.3] and in [27, §5]. We do not repeat this process here. We then set  $U^{(k)} = \operatorname{argmin}_{V \in H} J^{(k)}(V)$ .

The scripts for other steps of Algorithm 1 can be written easily.

**Remark 5.3.** We choose  $\lambda, \beta$  in the Carleman Weight Function defined in 2.1 by a trial-error process that is similar to the one in [25]. Just as in [25], we choose a reference numerical test in which we know the true solution (Test 1 in section 5.3). We then tried several values of  $\lambda, \beta$  until obtained a satisfactory numerical result for that reference test. Next, we have used the same values of these parameters for all other tests. In our computation,  $\lambda = 40, \beta = 20$ .

### 5.3 Numerical results

In this section, we present three (3) numerical tests to verify the efficiency of Algorithm 1. The noise level of the data in these tests is 20%.

**Test 1.** In this test, the source function is defined as follows

$$p_{\text{true}} = \begin{cases} 8 & 0.2x^2 + (y - 0.2)^2 < 0.25^2, \\ 0 & \text{otherwise.} \end{cases}$$

The function  $F$  has the form of

$$F(s, \mathbf{p}) = s + \sqrt{p}$$

The true and the reconstructed source function,  $p^*$  and  $p_{\text{comp}}$  respectively, are displayed in Figure 2. The true source includes an ellipse placed at point  $(x, y) = (0, 0.2)$  with contrast 8, see 2a. It is evident that our numerical method can successfully reconstruct the source function with a fast convergence. In more details, Figure 2b shows the computed source function which clearly indicates the position of the ellipse. The maximal value of the inclusion is 8.5022 (relative error 6.28%). Although the contrast is high, our method provides a good approximation of the true source without requesting a good initial solution. Besides, Figure 2c illustrates the consecutive relative errors which are computed as follows

$$\text{err}_k = \frac{\|p^{(k)} - p^{(k-1)}\|_{L^\infty(\Omega)}}{\|p^{(k)}\|_{L^\infty(\Omega)}} \quad \text{for } k = 1, 2, \dots, 8$$

It is noticeable that our numerical method converges rapidly. The consecutive errors go to zero quickly. Actually, after only five (5) iterations, we can obtain a stable solution for the source function. This fact verifies numerically the rate of convergence estimate  $O(\theta^n)$  as  $n \rightarrow \infty$  in (4.12) and (4.25).

**Test 2.** In this test, the source function is defined as follows

$$p_{\text{true}} = \begin{cases} 6 & (x + 0.5)^2 + (y + 0.5)^2 < 0.35^2, \\ 8 & (x + 0.5)^2 + (y - 0.5)^2 < 0.35^2, \\ 10 & (x - 0.5)^2 + (y + 0.5)^2 < 0.35^2, \\ 0 & \text{otherwise.} \end{cases}$$

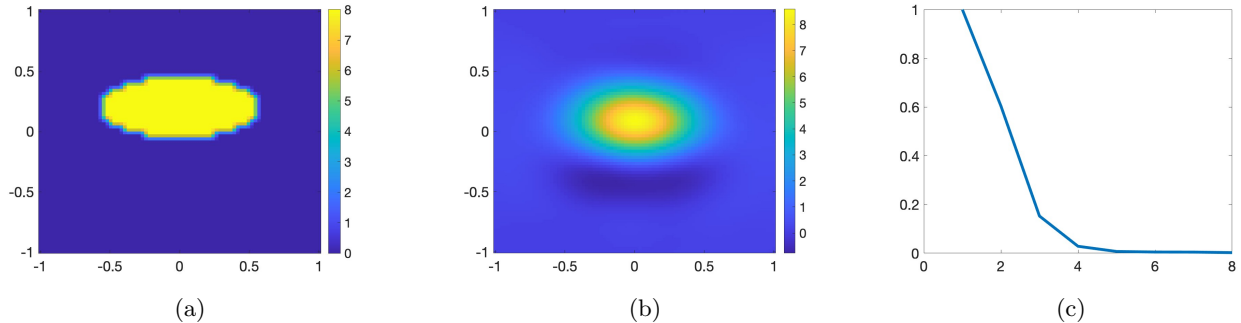


Figure 2: Test 1. The reconstruction of the source function. The initial solution of the source function  $p^{(0)}(\mathbf{x}) = 0, \forall \mathbf{x} \in \Omega$ . (a) The function  $p_{\text{true}}$ . (b) The computed source function  $p_{\text{comp}}$  obtained by Step 6 of Algorithm 1. (c) The consecutive relative error  $\frac{\|p^{(k)} - p^{(k-1)}\|_{L^\infty(\Omega)}}{\|p^{(k)}\|_{L^\infty(\Omega)}}$  for  $k = 1, 2, \dots, 8$ . The noise level of the data in this test is 20%.

The function  $F$  has the form of

$$F(s, \mathbf{p}) = s(1 - s) + \frac{1}{2} (|p_1| - |p_2|)$$

The true and the reconstructed source function,  $p^*$  and  $p_{\text{comp}}$  respectively, are displayed in Figure 3. The true source includes three ball with different contrasts, see 3a. The computed source function in Figure 3b clearly indicates the position of balls and it is a good approximation of the true one. The upper left ball has the true value 8 and the maximal computed one 8.3344 (relative error 4.18%). The lower left ball has the true value 6 and the maximal computed one 6.2892 (relative error 4.82%). The lower right ball has the true value 10 and the maximal computed one 11.0032 (relative error 10.03%). Besides, the Figure 2c illustrates our numerical method converges rapidly after only five (5) iterations.

**Test 3.** In this test, the source function is defined as follows

$$p_{\text{true}} = \begin{cases} 1 & 0.4^2 < x^2 + y^2 < 0.8^2, \\ 0 & \text{otherwise.} \end{cases}$$

The function  $F$  has the form of

$$F(s, \mathbf{p}) = \sqrt{p_1^2 + p_2^2} + 1$$

The true and the reconstructed source function,  $p^*$  and  $p_{\text{comp}}$  respectively, are displayed in Figure 4. The true source includes a ring with contrast 1, see 4a. The Figure 4b shows the computed source function which clearly indicates the position of the ring and the void inside. The maximal value of the ring is 0.9226 (relative error 7.74%). Besides, the consecutive relative errors in the Figure 2c illustrates the fast convergence of our numerical method. The convergence is obtained after seven (7) iterations.

## 6 Concluding remarks

In this paper, we introduce a new iterative method to solve an inverse source problem for a nonlinear parabolic equations. The first step of our numerical method is to derive a system of nonlinear elliptic

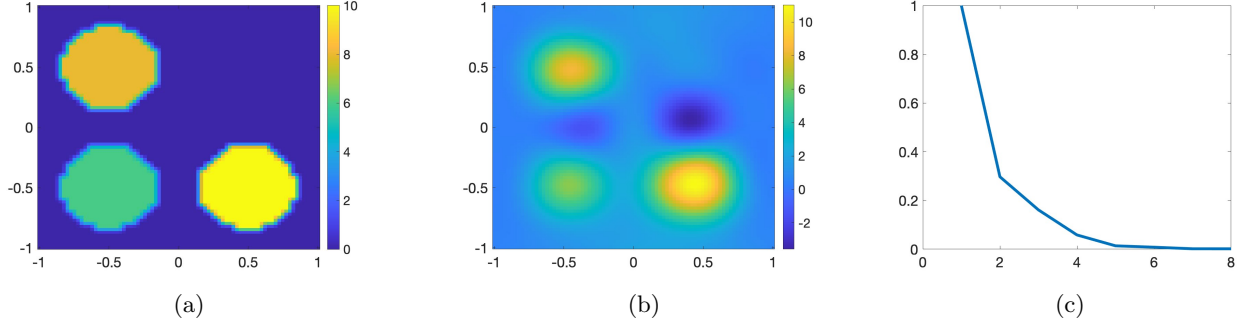


Figure 3: Test 2. The reconstruction of the source function. The initial solution of the source function  $p^{(0)}(\mathbf{x}) = 0, \forall \mathbf{x} \in \Omega$ . (a) The function  $p_{\text{true}}$ . (b) The computed source function  $p_{\text{comp}}$  obtained by Step 6 of Algorithm 1. (c) The consecutive relative error  $\frac{\|p^{(k)} - p^{(k-1)}\|_{L^\infty(\Omega)}}{\|p^{(k)}\|_{L^\infty(\Omega)}}$  for  $k = 1, 2, \dots, 8$ . The noise level of the data in this test is 20%.

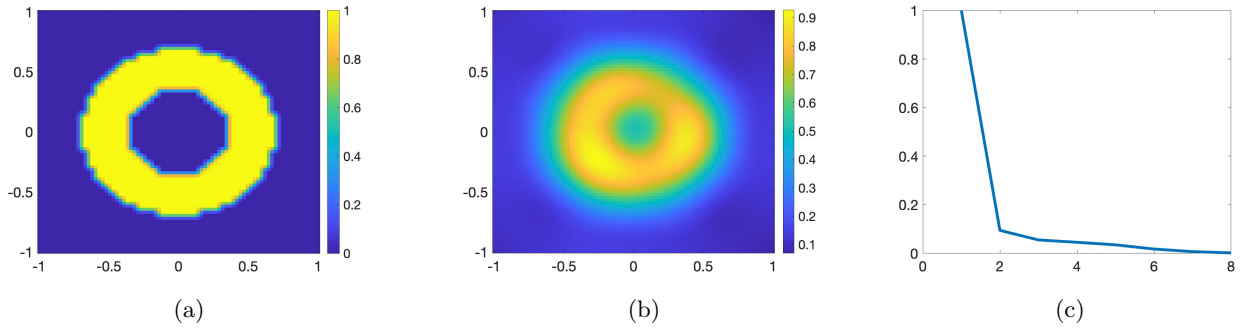


Figure 4: Test 3. The reconstruction of the source function. The initial solution of the source function  $p^{(0)}(\mathbf{x}) = 0, \forall \mathbf{x} \in \Omega$ . (a) The function  $p_{\text{true}}$ . (b) The computed source function  $p_{\text{comp}}$  obtained by Step 6 of Algorithm 1. (c) The consecutive relative error  $\frac{\|p^{(k)} - p^{(k-1)}\|_{L^\infty(\Omega)}}{\|p^{(k)}\|_{L^\infty(\Omega)}}$  for  $k = 1, 2, \dots, 8$ . The noise level of the data in this test is 20%.

equations whose solutions yields directly the solution for the inverse source problem. We then propose an iterative scheme to solve that nonlinear system. Our numerical method is global convergent in the sense that:

- (i) It provides a good approximation to the true source function.
- (ii) It does not require any knowledge of the true source function. This means a good initial guess is not necessary.

In our computation, we start our iterative scheme from the zero vector. The convergence of our scheme was proved rigorously. Numerical results are present to verify our theoretical part.



**Acknowledgment.** The author sincerely appreciates Dr. Loc H. Nguyen for many fruitful discussions that strongly improve the mathematical results and the presentation of this paper.

This work was partially supported by US Army Research Laboratory and US Army Research Office grant W911NF-19-1-0044, by National Science Foundation grant DMS-2208159, and by funds provided by the Faculty Research Grant program at UNC Charlotte Fund No. 111272.

## References

- [1] A. El Badia and T. Ha-Duong. On an inverse source problem for the heat equation. application to a pollution detection problem. *Journal of Inverse and Ill-posed Problems*, 10:585–599, 2002.
- [2] A. B. Bakushinskii, M. V. Klibanov, and N. A. Koshev. Carleman weight functions for a globally convergent numerical method for ill-posed Cauchy problems for some quasilinear pdes. *Nonlinear Anal. Real World Appl*, 34:201–224, 2017.
- [3] L. Beilina and M. V. Klibanov. *Approximate Global Convergence and Adaptivity for Coefficient Inverse Problems*. Springer, New York, 2012.
- [4] A. L. Bukhgeim and M. V. Klibanov. Uniqueness in the large of a class of multidimensional inverse problems. *Soviet Math. Doklady*, 17:244–247, 1981.
- [5] T. Carleman. Sur les systemes lineaires aux derivees partielles du premier ordre a deux variables. *C. R. Acad. Sci. Paris*, 197:471–474, 1933.
- [6] M. V. Klibanov. Global convexity in a three-dimensional inverse acoustic problem. *SIAM Journal on Mathematical Analysis*, 28(6):1371–1388, 1997.
- [7] M. V. Klibanov. Estimates of initial conditions of parabolic equations and inequalities via lateral Cauchy data. *Inverse Problems*, 22:495–514, 2006.
- [8] M. V. Klibanov. Carleman estimates for the regularization of ill-posed Cauchy problems. *Applied Numerical Mathematics*, 94:46–74, 2015.
- [9] M. V. Klibanov. Convexification of restricted Dirichlet to Neumann map. *J. Inverse and Ill-Posed Problems*, 25(5):669–685, 2017.
- [10] M. V. Klibanov and O. V. Ioussoupova. Uniform strict convexity of a cost functional for three-dimensional inverse scattering problem. *SIAM Journal on Mathematical Analysis*, 26(1):147–179, 1995.
- [11] M. V. Klibanov and A. E. Kolesov. Convexification of a 3-D coefficient inverse scattering problem. *Computers & Mathematics with Applications*, 77(6):1681–1702, 2019.
- [12] M. V. Klibanov, A. E. Kolesov, and D-L. Nguyen. Convexification method for an inverse scattering problem and its performance for experimental backscatter data for buried targets. *SIAM Journal on Imaging Sciences*, 12(1):576–603, 2019.
- [13] M. V. Klibanov, A. E. Kolesov, A. Sullivan, and L. Nguyen. A new version of the convexification method for a 1D coefficient inverse problem with experimental data. *Inverse Problems*, 34(11):115014, 2018.

- [14] M. V. Klibanov, T. T. Le, and L. H. Nguyen. Numerical solution of a linearized travel time tomography problem with incomplete data. *SIAM Journal on Scientific Computing*, 42(5):B1173–B1192, 2020.
- [15] M. V. Klibanov, T. T. Le, L. H. Nguyen, A. Sullivan, and L. Nguyen. Convexification-based globally convergent numerical method for a 1D coefficient inverse problem with experimental data. *Inverse Problems and Imaging*, 0:–, 2021.
- [16] M. V. Klibanov and J. Li. *Inverse Problems and Carleman Estimates: Global Uniqueness, Global Convergence and Experimental Data*. De Gruyter, 2021.
- [17] M. V. Klibanov, J. Li, and W. Zhang. Convexification for the inversion of a time dependent wave front in a heterogeneous medium. *SIAM Journal on Applied Mathematics*, 79(5):1722–1747, 2019.
- [18] M. V. Klibanov, J. Li, and W. Zhang. Convexification of electrical impedance tomography with restricted Dirichlet-to-Neumann map data. *Inverse problems*, 35(3):035005, 2019.
- [19] M. V. Klibanov, J. Li, and W. Zhang. Convexification for an inverse parabolic problem. *Inverse Problems*, 36(8):085008, 2020.
- [20] M. V. Klibanov and L. H. Nguyen. Pde-based numerical method for a limited angle X-ray tomography. *Inverse Problems*, 35(4):045009, 2019.
- [21] O. A. Ladyzhenskaya, V. A. Solonnikov, and N. N. Ural'tseva. *Linear and quasilinear equations of Parabolic Type*, volume 23. American Mathematical Society, Providence, RI, 1968.
- [22] R. Lattes and J-L. Lions. The method of quasi-reversibility: applications to partial differential equations. Technical report, 1969.
- [23] M. M. Lavrent'ev, V. G. Romanov, and Shishat'skii. *Ill-Posed Problems of Mathematical Physics and Analysis*. Translations of Mathematical Monographs. AMS, Providence: RI, 1986.
- [24] T. T. Le, M. V. Klibanov, L. H. Nguyen, A. Sullivan, and L. Nguyen. Carleman contraction mapping for a 1D inverse scattering problem with experimental time-dependent data. *Inverse Problems*, 38(4):045002, feb 2022.
- [25] T. T. Le and L. H. Nguyen. A convergent numerical method to recover the initial condition of nonlinear parabolic equations from lateral cauchy data. *Journal of Inverse and Ill-posed Problems*, 2020.
- [26] T. T. Le and L. H. Nguyen. The gradient descent method for the convexification to solve boundary value problems of quasi-linear pdes and a coefficient inverse problem. *arXiv preprint arXiv:2103.04159*, 2021.
- [27] T. T. Le, L. H. Nguyen, T-P. Nguyen, and W. Powell. The Quasi-reversibility method to numerically solve an inverse source problem for hyperbolic equations. *Journal of Scientific Computing*, 87(90), 2021.
- [28] J. Li, M. Yamamoto, and J. Zou. Conditional stability and numerical reconstruction of initial temperature. *Communications on Pure and Applied Analysis*, 8:361–382, 2009.

- [29] Q. Li and L. H. Nguyen. Recovering the initial condition of parabolic equations from lateral Cauchy data via the quasi-reversibility method. *Inverse Problems in Science and Engineering*, pages 580–598, 2019.
- [30] D-L. Nguyen, L. H. Nguyen, and T. Truong. The Carleman-based contraction principle to reconstruct the potential of nonlinear hyperbolic equations. *preprint arXiv:arXiv:2204.06060*, 2022.
- [31] H-M. Nguyen and L. H. Nguyen. Cloaking using complementary media for the Helmholtz equation and a three spheres inequality for second order elliptic equations. *Transaction of the American Mathematical Society*, 2:93–112, 2015.
- [32] L. H. Nguyen. A new algorithm to determine the creation or depletion term of parabolic equations from boundary measurements. *Computers & Mathematics with Applications*, 80(10):2135–2149, 2020.
- [33] L. H. Nguyen. The Carleman-contraction method to solve quasi-linear elliptic equations. *arXiv preprint arXiv:2203.12694*, 2022.
- [34] L. H. Nguyen and M. V. Klibanov. Carleman estimates and the contraction principle for an inverse source problem for nonlinear hyperbolic equations. *Inverse Problems*, 38(3):035009, feb 2022.
- [35] L. H. Nguyen, Q. Li, and M. V. Klibanov. A convergent numerical method for a multi-frequency inverse source problem in inhomogenous media. *Inverse Problems and Imaging*, 13:1067–1094, 2019.
- [36] M. H. Protter. Unique continuation for elliptic equations. *Trans. Amer. Math. Soc.*, 95:81–91, 1960.
- [37] A. V. Smirnov, M. V. Klibanov, and L. H. Nguyen. On an inverse source problem for the full radiative transfer equation with incomplete data. *SIAM Journal on Scientific Computing*, 41(5):B929–B952, 2019.
- [38] K. A. Vo, G. W. Bidney, M. V. Klibanov, L. H. Nguyen, L. Nguyen, A. J. Sullivan, and V. N. Astratov. Convexification and experimental data for a 3D inverse scattering problem with the moving point source. *Inverse Problems*, 36(8):085007, 2020.
- [39] K. A. Vo, G. W. Bidney, M. V. Klibanov, L. H. Nguyen, L. Nguyen, A. J. Sullivan, and V. N. Astratov. An inverse problem of a simultaneous reconstruction of the dielectric constant and conductivity from experimental backscattering data. *Inverse Problems in Science and Engineering*, 29(5):712–735, 2021.
- [40] K. A. Vo, M. V. Klibanov, and L. H. Nguyen. Convexification for a three-dimensional inverse scattering problem with the moving point source. *SIAM Journal on Imaging Sciences*, 13(2):871–904, 2020.